



# Adhesion enhancement of sol–gel coating on polycarbonate by heated impregnation treatment

Linda Y.L. Wu<sup>a,\*</sup>, L. Boon<sup>b</sup>, Z. Chen<sup>b</sup>, X.T. Zeng<sup>a</sup>

<sup>a</sup> Singapore Institute of Manufacturing Technology, 71 Nanyang Drive, Singapore 638075, Singapore

<sup>b</sup> School of Materials Science and Engineering, Nanyang Technological University, 50 Nanyang Avenue, Singapore 639798, Singapore

## ARTICLE INFO

Available online 20 March 2009

### Keywords:

Adhesion  
Impregnation  
Sol–gel  
Coating  
Scratch resistance  
Hardness

## ABSTRACT

The main limitation in using coated plastics for optical components, electronic applications and display systems is the softness of the substrate surfaces, which is responsible for the low impact and abrasion resistance and weak adhesion between the coating and the substrate. In this paper, we report a new strategy for surface pre-treatment of plastics using heated vacuum equipment and sol–gel materials to provide both chemical bonds and penetrated hard layer into the plastic surface to increase the overall performance of the coated plastic components. The heated vacuum treatment process involves: (1) surface cleaning and pore opening by heating and vacuum conditions, (2) impregnation of hydrolyzed hybrid precursor into polymer substrate under pressure and elevated temperature, (3) aminolysis of diffused precursor with surface to form chemical bonds and hardened surface layer, (4) formation of chemical bonds at treated surface with sol–gel hard coating. An impregnation depth of 1.5  $\mu\text{m}$  was detected. Water contact angle dropped to below 40° and roughness increased after treatment. These provided better adhesion by increased wettability and contact area. Much increased nanoindentation hardness and Young's modulus after impregnation provided a gradient in mechanical properties between soft substrate and hard sol–gel coating. The hardened substrate delays the plastic deformation in substrate during pencil scratch test, thereby preventing early gouge failure. Both the better adhesion and the delayed gouge failure contributed to the increased scratch resistance from 6B to 8H after sol–gel coating.

© 2009 Elsevier B.V. All rights reserved.

## 1. Introduction

Transparent polymer materials such as polycarbonate (PC) have excellent transparency and lower density than inorganic glasses and have been used to replace glasses in a wide range of applications, such as display panels of electronic devices, compact disks, lightweight eyewear lenses and safety windows [1,2]. Despite their excellent physical and optical properties, the poor scratch and abrasion resistance and the reduction in transparency during use has hindered their applications [3–6].

A hard and scratch-resistant protective coating is needed in order to improve the surface characteristics while capitalizing on their desirable bulk properties. In the past decade, inorganic–organic hybrid materials prepared by sol–gel route have been extensively explored [7–13], since they offer the prospect of combining the mechanical toughness and flexibility of the organic component with the hardness and thermal stability of the inorganic component. Industrial applications have demonstrated the formation of wear and

abrasion resistant coatings on engineering plastics such as the headlights of cars made from PC, side windows in buses made from PMMA, and scratch-resistant coatings on ophthalmic.

Despite of some successful applications, it is still challenging to achieve satisfactory overall performance of a coated plastic component in heavy loading and harsh environment. The instability of adhesive bonding at the interface between coating and the polymeric substrate and the low durability under abrasion and wear conditions inspired this research on a new strategy to enhance both the chemical bonding and the interfacial strength. Polymer surfaces do not have the necessary reactive hydroxyl groups present on metal or ceramic substrates. In many instances, it is necessary to pre-treat the surface of the polymer to increase the adhesion characteristics. A variety of surface treatment techniques have been extensively studied. For example, (1) plasma treatment to remove the organic contaminations, change the surface polarity and activate the surface for better wetting and adhesion [14–16], (2) applying silane adhesion promoters or silane coupling agents to form copolymerized interface and improves adhesion [17–20], (3) wet chemical etching by hydrogen peroxide–sulphuric acid ( $\text{H}_2\text{O}_2$ – $\text{H}_2\text{SO}_4$ ) solution to introduce hydroxyl groups and increase oxygen content on the polymer surface for bonding with partially hydrolyzed tetraethyl orthosilicate (TEOS), (4) wet chemical etching by potassium permanganate solution to increase the adhesion through roughening of the

\* Corresponding author. Tel.: +65 67938999; fax: +1 65 67916377.  
E-mail address: [ylwu@simtech.a-star.edu.sg](mailto:ylwu@simtech.a-star.edu.sg) (L.Y.L. Wu).

substrate by the etching agent [21], (5) silicon alkoxide impregnation on polyester surface using tetramethoxysilane (TMOS):ethanol solution to form Si–O–Si bonds at the interface, and enhance chemical interlocking with sol–gel coating [7]. Each of the treatment has its limitations; either only changes the chemical groups on surface (methods 1, 2, 3) or only roughens the surface (method 4) without improving the mechanical properties. Method (5) could induce some penetration, but the depth is very small (100 nm). In this paper, we report a new treatment strategy that combines all the advantages of the above methods with additional vacuum cleaning in the first step and applied pressure in the impregnation step, in order to achieve both chemical bonds and interpenetrated hardened interfacial layer for both strong adhesion and a gradient interfacial layer to reduce the mismatch of mechanical and thermal properties between the sol–gel coating and the polymer substrate.

## 2. Experimental details

### 2.1. Substrate preparation

Polycarbonate substrates, measured 100 mm × 50 mm × 3 mm, were supplied with a layer of protective film, which was peeled off before the substrate was washed in isopropanol (IPA), and boiled in IPA for 5 min. The purpose of washing in IPA is to degrease the surface and remove any impurities that may affect the impregnation quality.

### 2.2. Materials

The following materials were purchased from qualified chemical suppliers and used without further purification: 3-glycidoxypropyl trimethoxysilane (GLYMO), tetraethylorthosilicate (TEOS), ethanol (EtOH), colloidal silica solution (Ludox AS-40), ethylenediamine (EDA), 3-aminopropyltriethoxysilane (APS), methyltrimethoxysilane (MTMS), ethyl methyl ketone (MEK), acetic acid (HAc), itaconic acid (Hit).

### 2.3. Formulation of hybrid precursor solution and sol–gel coating solution

After studied several organosilanes in different compositions, we found that the best precursor solution was composed of the following components (in molar ratio): MTMS:APS:EtOH:MEK:H<sub>2</sub>O:HAc = 1.0:1.0:14.0:4.0:6.0:0.4. MTMS was hydrolysed in water, ethanol and acetic acid. APS was also hydrolysed first in water, then MEK was added. Then the two solutions were mixed and stirred for at least 2 h. Further dilution by ethanol was carried out to ensure the solution is not too viscous resulting in non-uniform layer thickness.

The sol–gel coating formulation has been reported in our earlier publication [22]. In short, a stock solution of GLYMO-TEOS was prepared by hydrolyzing them in ethanol and water in an acidic solution. The molar ratios of the components were: GLYMO:TEOS:EtOH:H<sub>2</sub>O:Hit = 1:1.63:2.19:5:0.26. The GLYMO and TEOS were hydrolysed separately and then mixed together and stirred for 24 h. To this mixture solution (A), a colloidal silica solution (Ludox AS-40) was first acidified to pH 3, and then added as hard filler in volume ratios of 30%. Just before the dip coating process, 0.05 wt.% of ethylenediamine (EDA) was added to the coating solution as the cross-linking agent of the epoxy ring in GLYMO.

### 2.4. Heated impregnation treatment process

The heat impregnation treatment process was carried out in a home-made heated vacuum chamber with adjustable and controllable temperature, vacuum, solution dosing speed and nitrogen pressure. The process parameters are briefly shown in Fig. 1. The procedures of the treatment process are: (1) load cleaned sample on stage which has a declined angle of 15° to the horizon, (2) close the

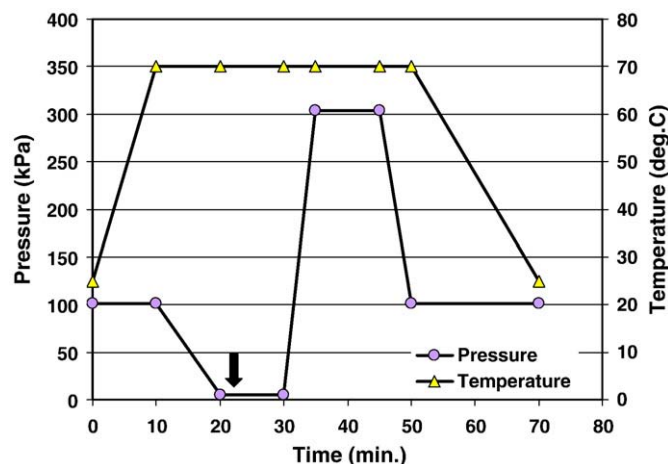


Fig. 1. Heated vacuum impregnation process parameters and procedures (dosing of precursor solution was done at 20 min).

chamber and tighten all the screws, (3) adjust temperature to 60, 70 or 80 °C and wait till the temperature reaches the set temperature, (4) switch on the vacuum till pressure drops to about zero and hold for 10 to 20 min, (5) turn on the dosing switch to inject the hybrid precursor solution onto the sample surface till the entire surface has been covered, (6) turn on the N<sub>2</sub> gas switch and open the valve till the pressure increases to 3 bar, (7) hold for 5, 10, 15 or 30 min to force the solution to impregnate into the substrate, (8) switch off the N<sub>2</sub> gas, and open the dosing knob to force out the remaining solution in the tubing so as to prevent clotting, (9) lower the temperature to room temperature and open the chamber for cooling for 10 min, (10) clean the chamber and switch off the power. The treated sample was further dried in oven at 80 °C for 1 h and was ready for sol–gel coating.

### 2.5. Coating process and characterization

The pre-treated PC substrates were dip coated with the prepared sol–gel coating solution in different withdrawal speeds to investigate the adhesion, and further coated with second layer and third layer to study the effect of total layer thickness on coating's hardness and scratch resistance. A curing step and an oxygen plasma treatment were carried out before the subsequent layer was applied. This is to avoid merging of the two layers and cracking upon curing due to too much shrinkage. After each dip coating, the specimens were placed in a bench top furnace for drying and curing. The drying was at 80 °C for 40 min. and curing at 110 °C for 90 min.

To investigate the chemical bonds on surface before and after the impregnation and sol–gel coating, Infrared absorption spectra of the modified surface and coatings were analyzed by Fourier-transformed infrared spectrometer (FTIR, Bio-Rad Excalibur Series FTS 3000) using the attenuated total reflectance (ATR, with Ge crystal) method. The thickness of the treated layer and coating layers were measured using a stylus profilometer (Talysurf Series 2 Stylus Profilometer) across the uncoated and coated areas on the same specimen. The adhesion between coating layer and substrate was assessed using the cross-cut tape test according to ASTM D 3359-02 [23] standard test method. The quality of adhesion was determined by comparing the cross-cut to the standard grading from 5B, 4B, 3B, 2B, 1B and 0B in decreasing adhesion. The surface roughness and water contact angle of the surfaces after treatment and sol–gel coating were measured by profilometer and an automatic video contact angle system (VCA Optima, VCA-2500XE, AST products, Inc). The image of the water drop is obtained when a pre-determined amount of water (0.5 μl) is dropped on the surface under test. The program then analyses the image of the drop and gives the contact angle value. The adhesion and

treatment layers were also analysed by optical microscopy (ZEISS Axiotron 2 CSM Vis–UV Inspection Microscope) and scanning electron microscope (ZEISS EVO<sup>®</sup>50 low vacuum scanning electron microscopy) on the top view and cross-section of the specimen.

The scratch resistance (or pencil hardness) of the coating was characterized by a commercial pencil hardness tester (Scratch Hardness Tester Model 291, ERICHSEN TESTING EQUIPMENT). The test conforms to ASTM Standard D3360-00 [24], where a vertical force

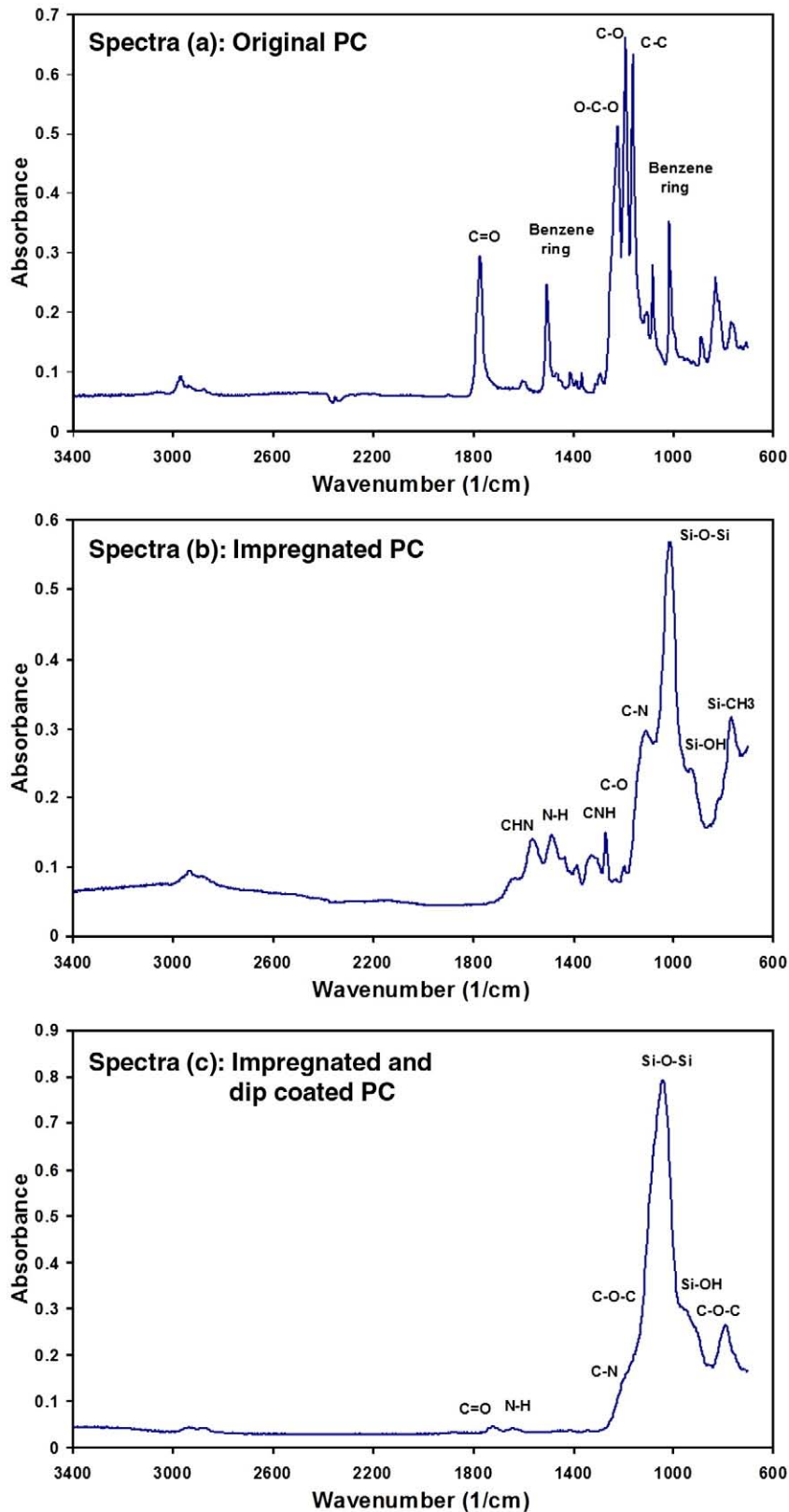


Fig. 2. FTIR spectra of original PC surface (a), impregnated PC surface (b), impregnated and sol-gel coated surface (c), showing chemical changes of the surface.

of  $7.5 \pm 0.1$  N was applied at  $45^\circ$  angle to the horizontal film surface as the pencil is moved over the coated surface. The grades from the softest to the hardest are: 6B-5B-4B-3B-2B-B-HB-F-H-2H-3H-4H-5H-6H-7H-8H-9H. Nano-indentation hardness and Young's modulus of the coatings were measured using a nano-indenter (NanoTest™). A Berkovitch tip (with a three-sided pyramid geometry) was employed. The load was controlled below 0.5 mN and the depth of the indentation was controlled to be less than 1/10 of the coating thickness in order to minimize the effect due to the substrate. The resultant displacement of the indenter into the surface is monitored with a sensitive capacitive transducer and displayed in real time as a function of load. The hardness and elastic modulus are then calculated by the established equations [25] by the software.

### 3. Results and discussion

#### 3.1. Chemical analyses

Fig. 2 shows the FTIR spectra of (a) original PC surface, (b) surface after impregnation, and (c) surface after one layer sol-gel coating. All the absorption peaks are labeled with the wavelength values, from which, the differences in chemical bonds can be identified. From spectra in Fig. 2(a), the more significant peaks are attributed to structural backbone of PC. Major groups are  $\text{O}-\text{C}-\text{O}$  at  $1222 \text{ cm}^{-1}$  ( $\text{O}-\text{C}-\text{O}$  stretching) and  $1768 \text{ cm}^{-1}$  ( $\text{C}=\text{O}$  stretching), benzene ring stretching at  $1502 \text{ cm}^{-1}$  and  $1014 \text{ cm}^{-1}$ ,  $\text{C}-\text{O}$  stretching at  $1190 \text{ cm}^{-1}$ , and  $\text{C}-\text{C}$  deformation at  $1161 \text{ cm}^{-1}$ .

Comparing the FTIR spectra of the impregnated surface (Fig. 2(b)) to the original PC, there is a shift in the major peaks, indicating an obvious surface reaction after impregnation. The most significant peak at  $1012 \text{ cm}^{-1}$  is assigned to the combination of siloxane ( $\text{Si}-\text{O}-\text{Si}$ ) and

para-substituent of the benzene ring. The presence of  $\text{Si}-\text{O}-\text{Si}$  indicates that some of the hydrolyzed APS and MTMS had undergone condensation among themselves. The higher absorbance peak at  $769 \text{ cm}^{-1}$  as compared to spectra (a) is attributed to the  $\text{Si}-\text{CH}_3$  bond due to MTMS. The weak narrow peak at  $920 \text{ cm}^{-1}$  ( $\text{Si}-\text{OH}$ ) is from the hydrolysed APS and MTMS as the coating was not fully cured before sol-gel coating. The weak peaks of amine group at  $822 \text{ cm}^{-1}$  ( $\text{N}-\text{H}$  bend) and  $1112 \text{ cm}^{-1}$  ( $\text{C}-\text{N}$  stretching) infer that most of the amine group in APS has cleaved the chains of PC into two chains [20]. One chain terminated with a phenol group at  $1196 \text{ cm}^{-1}$  ( $\text{C}-\text{O}$  stretching) and  $1383 \text{ cm}^{-1}$  ( $\text{O}-\text{H}$  bending) and the other with a urethane group ( $\text{R}-\text{NHCOO}-\text{R}$ ) at band  $1560 \text{ cm}^{-1}$  ( $\text{CHN}$  bending). Further possible evident of urethane group is the existent of the amide group at  $1483 \text{ cm}^{-1}$  ( $\text{N}-\text{H}$  bending),  $1318 \text{ cm}^{-1}$  ( $\text{C}-\text{N}$  stretching) and  $1268 \text{ cm}^{-1}$  (combination of  $\text{C}-\text{N}$  stretching and  $\text{N}-\text{H}$  bending). These peaks fall in the same range (from  $1295 \text{ cm}^{-1}$  to  $1596 \text{ cm}^{-1}$ ) as some of the structural backbone of the PC, thereby giving a few broader peaks. Peaks at  $1768 \text{ cm}^{-1}$  and  $1222 \text{ cm}^{-1}$  in spectra (a) are also not present in spectra (b). This explains the absence of the  $\text{O}-\text{C}-\text{O}$  group due to the cleaving of PC chains by APS.

With the addition of the dip coating layer on top of the heat treated surface, the spectra (c) in Fig. 2 appears different. Comparing to spectra (b), the structural backbone has a higher  $\text{Si}-\text{O}-\text{Si}$  stretching vibration at  $1038 \text{ cm}^{-1}$  due to the hydrolysis and condensation of the alkoxy silane groups leading to much more  $\text{Si}-\text{O}-\text{Si}$  bonds. The shoulder peak at  $902 \text{ cm}^{-1}$  ( $\text{C}-\text{O}-\text{C}$  asymmetric stretching) infers that little epoxy ring is present and it can be deduced that the EDA act as a cross linking agent to open up the epoxy ring and form a tertiary amine ( $\text{C}-\text{N}$  stretching) and secondary alcohol at  $1200 \text{ cm}^{-1}$  [2]. There are little peak at  $1718 \text{ cm}^{-1}$  because of the minimal detection of  $\text{C}=\text{O}$  bond embedded beneath the coating layer.

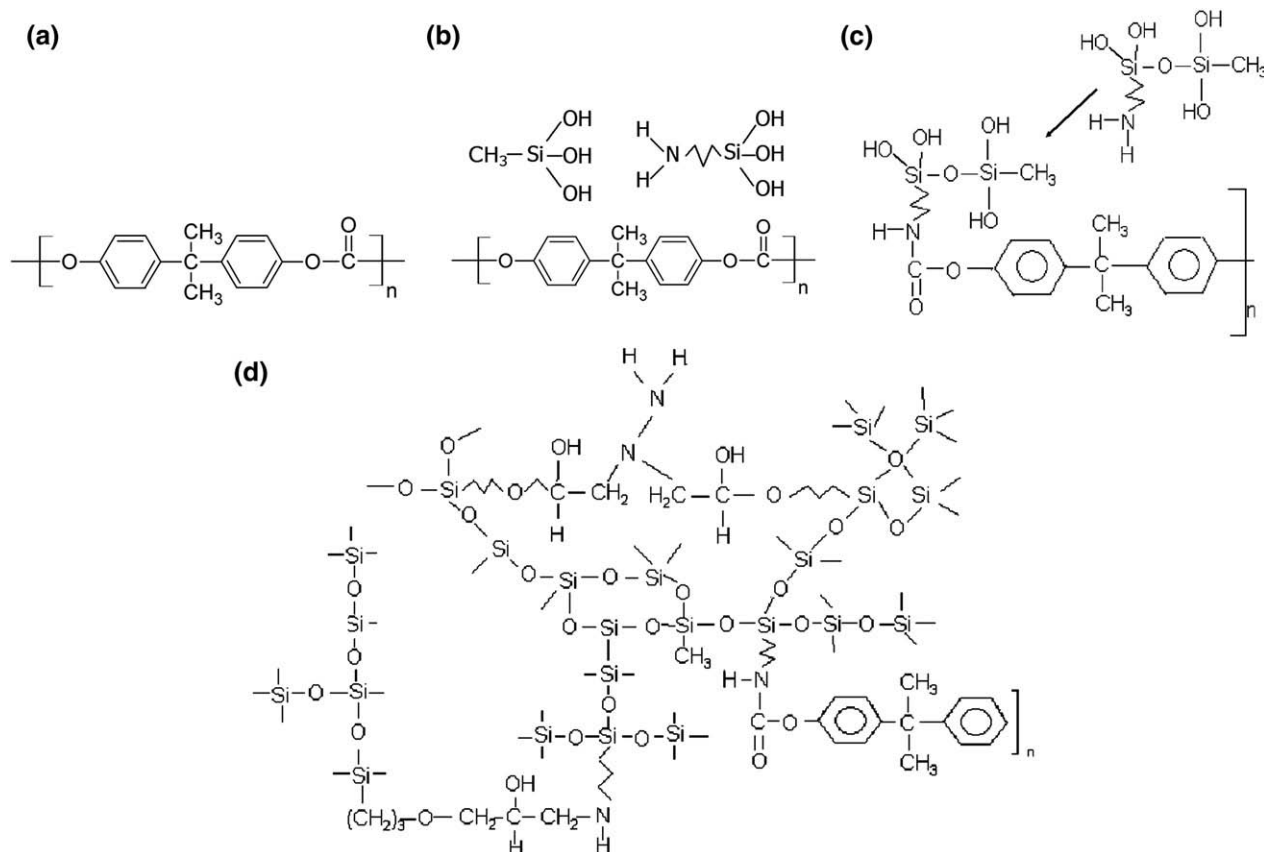


Fig. 3. Schematic diagrams depicting original PC (a), diffusion and interpenetration of hydrolyzed hybrid precursor within the polycarbonate substrate (b), aminolysis reaction of substrate to form urethane linkage and some condensation reactions between hydrolyzed precursors (c), and surface condensation with subsequent sol-gel coating (d).

### 3.2. Adhesion mechanism and surface analyses

From the chemical analyses of the original PC and impregnated surface, the chemical reaction between the APS-MTMS hybrid precursor to PC substrate can be proposed and the adhesion mechanism can be deduced. Fig. 3(a) shows the original chemical structure of PC material. When the PC surface is immersed in the hydrolysed hybrid precursor solution at elevated temperature under 2 bar pressure, both chemical reaction and physical penetration of the precursors into the substrate are accelerated and enhanced. The hybrid precursor would first diffuse and interpenetrate into the PC surface, since the PC surface was already heated and possible pores were opened, and surface structure was expanded under the vacuum and elevated temperature. With the presence of the precursor, PC undergoes aminolysis whereby there was selective chain scission at the carbonate linkages and triethoxysilyl groups become chemically bonded to the substrate through urethane linkages [20], leaving the reactive hydroxyl groups at the surface for further reaction with the dip coating solution and some being condensed as shown Fig. 3(b, c). A similar study proved that the presence of hydroxylated species on surface after water-plasma treatment promoted the adhesion strength between a titania film to PC substrate by more than a factor of two [26]. When the modified PC was dip coated with the GLYMO/TEOS/EDA sol-gel solution, the hydroxyl groups present in the dip coating solution react with those present on the surface of the modified PC substrate to form a Si–O–Si network. Furthermore, the remaining unreacted amine from APS may also cross-link with GLYMO to increase the adhesion between the coating layer and the modified PC surface as shown in Fig. 3(d).

To evaluate the surface wettability after vacuum impregnation and sol-gel coating, the water contact angle and surface roughness were measured. Table 1 shows the results. It is seen that the contact angle dropped to below 40° after impregnation treatment indicating much better wettability and adhesion than un-treated PC. In fact, it was not possible to coat a uniform sol-gel layer directly to as-received PC due to non-wetting. A surface treatment is always necessary for PC. The surface roughness increased after impregnation treatment due to the formation of a porous layer resulting from the partially penetrated material into the PC. The microstructure of the surface and its effect on adhesion will be discussed in the next section.

### 3.3. Layer thickness and microstructure analyses

In order to examine the penetration of impregnated material in PC, cross-section of the coated samples were analysed by both optical microscope and SEM. The sample was mounted into epoxy/hardener material and polished by fine polishing cloth with 1 μm alumina polishing dispersion. Fig. 4 shows a SEM image of the cross-section of a sample treated by impregnation and coated by two dip sol-gel coating. As seen in the image, a uniform impregnated layer was formed directly on the PC surface. An average constant thickness of 5 μm was achieved (at least 5 measurements were performed). The average constant thickness was also measured by a profilometer. The measuring length covered the uncoated PC surface and the coated surface, showing a height difference of 3.5 μm between the original PC surface and the top surface of the impregnated layer. Taking the difference between these two average values, we obtained the

**Table 1**

Surface roughness and water contact angle values of original PC, impregnated surface and sol-gel coated surface.

Sample	Contact angle (°) <sup>a</sup>	Surface roughness (μm) <sup>a</sup>
Original PC	78 ± 5	0.11 ± 0.02
Impregnated PC surface	37 ± 3.5	0.29 ± 0.05
Sol-gel coated surface	89 ± 3.2	0.22 ± 0.04

<sup>a</sup> Each value is the average of five measurements on one sample.

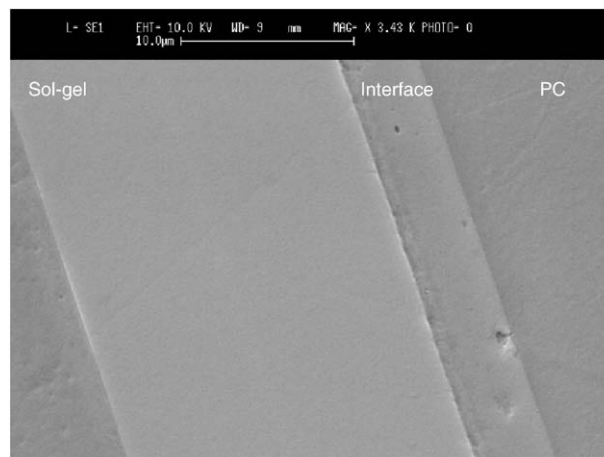


**Fig. 4.** SEM image of cross-section of impregnated PC surface with two dip sol-gel coating showing 5 μm thick impregnated layer and 20 μm thick sol-gel coating.

impregnation depth of approximately 1.5 μm. This depth is larger than most of the reported pre-treatment depths, which are typically below 100 nm [7].

There is an interfacial layer between the impregnated layer and the sol-gel dip coating layer. This indicates that a merge or interpenetration between the coating material and the impregnated layer had occurred. This is because that the impregnated layer was not fully cured (only dried at 80 °C for 1 h), the available hydroxyl groups could react and condense together with the dip coating material to form strong chemical bonding. This is the reason that we added MTMS into the impregnation material. Of course, this chemical bonding is not as perfect as the dip coating material itself; therefore, the interface looks less dense than the coating layer. The surface structure and mean roughness (Ra value) of the impregnated surface and sol-gel coated surface are shown in Fig. 5. The porous structure and rougher surface after impregnation contribute to the adhesion by providing larger contact area and anchoring effect between the coating and the substrate.

### 3.4. Scratch resistance and nano-indentation hardness

The impregnation treatment duration and temperature were varied to study the effects of these parameters on the coating's mechanical properties. Table 2 shows the pencil scratch grade measured and the respective optical transparency observed under optical microscope in relation to the process parameters. It is seen from Table 2 that temperature of 70 °C with nitrogen gas pressure maintained for 10 min gave a better scratch hardness and a thin transparent layer. An increased pencil grade from 6B to B has been achieved by the impregnation treatment. Higher temperatures resulted in rougher and non-uniform layer, therefore, is not preferred. The major reason for the hardness improvement by the heated impregnation is the penetration of the impregnation material into PC and excess layer condensed on the surface with strong chemical bonds. The hydrolyzed MTMS-APS formed integrated network from under layer of PC to the top of the modified surface, whereby improving the hardness of the substrate for further sol-gel coating. This provides a gradient in mechanical and thermal properties between the sol-gel hard coating and the soft PC substrate, whereby reduces the localized plastic deformation and delays the breaking of the surface layer by the pencil tip. In our earlier publication [22], we analysed the failure model of the sol-gel coating on PC under pencil scratch, which consisted of gouge failure under static pressure (causing plastic deformation in the complaint substrate) and film cracking under the sliding of pencil tip. We concluded that major factors influencing pencil scratch resistance are substrate hardness/

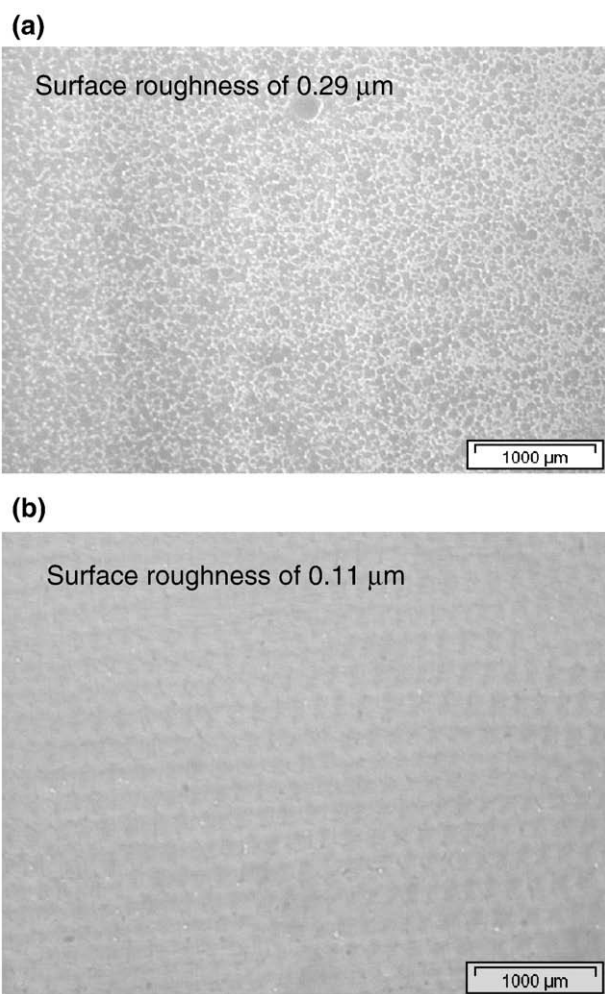


**Fig. 5.** Optical microscope images of top views of impregnated PC surface (a) and two dip sol-gel coated surface (b).

strength, coating thickness, and intrinsic properties of the coating material. A study on the cracking and decohesion of a similar sol-gel coating on metallic substrate [27] concluded that GTMS containing coating displayed a quasi-plastic response to fracture. This indicated that the plastic deformation leading to gouge failure is likely the major failure mode. In the current work, we confirmed that pencil scratch resistance can be effectively increased by the impregnation treatment, which increased both the hardness/strength of the substrate and the

**Table 2**

Pencil hardness and observed transparency of samples treated by different process parameters.

Vacuum (min)	Temp (°C)	N <sub>2</sub> gas pressure with solution (min)	Observations after drying at 80 °C for 30 min <sup>a</sup>	Pencil scratch grade
–	–	–	–	6B (original PC)
10	60	10	Transparent, with porosity	2B
10	60	5	Thin, transparent, smooth layer	2B
10	70	10	Thin, transparent, with porosity	B
10	70	5	Thin, transparent, smooth layer	2B
10	80	10	Transparent, rough surface	B
10	80	5	Smooth layer	2B
10	90	10	Thick, non-homogenous	B

<sup>a</sup> Observation by optical microscope.

**Table 3**

Pencil scratch grade and coating thickness of samples after treatment and multilayer coating.

Temp. (°C)	Pencil scratch grade/total coating thickness (μm)			
	Heat treatment	1 Dip coat layer	2 Dip coat layer	3 Dip coat layer
60	2B/8.4	F/19.8	2H/20.4	–
70	B/7.1	2H/10.7	8H/20.2	9H/31.3 with cracks
80	B/5.1	F/9.6	6H/14.05	–
Commercial lenses	HB	–	–	–
Plasma treated PC	H/12.7	–	4H/21.3	–

chemical bonding between coating and substrate. The observed porosity on the surface is due to the evaporation of the solvent during heat treatment and drying. This is beneficial to the adhesion between dip coating layer and the heat treated surface by providing larger contact area and anchoring effect.

After the impregnation treatment, the PC sample was dip coated with the sol-gel coating at a withdrawal speed of 10 in./min. The pencil scratch hardness increased as shown in Table 3. A commercial optical lens with a scratch resistance coating was tested as a benchmark. The direct coating on PC with oxygen plasma treatment was also tested and tabulated in Table 3. From the results obtained, it can be inferred that the dip coating material formed strong adhesion with the impregnated surface and provided hard coating for the PC. The best parameters of impregnation process are: 70 °C, pressure 3 bar, duration 10 to 30 min. With multi-layer thicker coating, the scratch resistance was also higher. Pencil hardness of 8H has been achieved on a two-layer coating sample. The second dip coating layer also showed smoother surface as compared to the first layer indicating higher cross linking of the inorganic and organic components. But with multi-layer coating up to the third layer, cracks were observed due to the shrinkage of coating material and strong capillary force exerted on the matrix in the course of drying [28]. When compared to the commercial lenses (with pencil scratch grade of HB), the pencil scratch grade of heat treated and dip coated PC is higher after first dip coating. The difference in thickness for the heat treatment at different temperatures is due to the higher evaporation of solvent at higher temperature. Comparing the two-layer coated impregnated sample to the plasma treated PC sample, the hardness was comparable after the first dip coating but was higher after the second dip coating. This further proved that the surface modification using the concept of pressure, temperature and duration to induce impregnation of the hybrid material into surface is a better pre-treatment for hard and durable coatings on PC substrate.

Adhesion quality was found to be 5B (0% removal), which is comparable to the commercial lens, while the hardness is much better than the commercial lens. Hardness and Young's modulus of the impregnated surface and the sol-gel coated surface were measured by nano-indentation and compared to plain polycarbonate [29]. The results are shown in Table 4. The improvements on both hardness and toughness of the surface are obvious after impregnation and after sol-gel coating. This proved that the impregnated layer provided a gradient layer between the sol-gel coating and the PC substrate reducing the mismatch in mechanical properties. Due to this hardened substrate and the chemical bonds formed, the resistance to gouge failure is increased; therefore, plastic deformation in substrate is delayed resulting in higher scratch resistance of the coated surface.

**Table 4**

Hardness and Young's modulus of original PC, impregnated layer and sol-gel coated layer.

Sample	Hardness, <i>H</i> (GPa)	Young's modulus, <i>E</i> (GPa)
Original PC <sup>a</sup>	0.0008	2.3–2.4
Impregnated PC	0.35 ± 0.04	4.98 ± 0.21
Sol-gel coated surface	0.95 ± 0.13	11.67 ± 1.6

<sup>a</sup> Values for original PC are from reference book [29].

#### 4. Conclusion

Polycarbonate surface has been treated by vacuum impregnation process under pressure and elevated temperature. The chemical composition of heat treatment solution has been optimized using MTMS/APTES hybrid precursors. Chemical bonds are formed through the cleavage of the carbonate group to obtain a strong urethane linkage, leaving attached hydroxyl groups at the surface. These hydroxyl groups then initiate surface condensation with the sol–gel coating (GPTS/TEOS/EDA) to form integrated network. An impregnation depth of approximately 1.5  $\mu\text{m}$  indicates a substantial penetration of the hybrid precursor into the polymer substrate. Reduced contact angle and increased roughness further ensure the wetting and anchoring effect for stronger adhesion. Increased hardness and Young's modulus after the pre-treatment provide hardened substrate for delayed plastic deformation and resistance to gouge failure leading to higher scratch resistance. Therefore, the high scratch resistance of the sol–gel coated PC attributes not only to the enhanced adhesion by chemical bonds and improved wetting and anchoring effect, but also to the hardened substrate which delayed the gouge failure under the scratch by a sharp tip. This transparent and scratch resistant coating achieved by surface modification can potentially remain durable against outdoor abrasion and sun exposure, therefore, is suitable for applications in automotive, aerospace and building industries.

#### References

- [1] C. Charitidis, A. Laskarakis, S. Kassavetis, C. Gravalidis, S. Logothetidis, *Superlattices Microstruct.* 36 (2004) 171.
- [2] G. Schottner, *Chem. Mater.* 13 (10) (2001) 3422.
- [3] J.H. Lee, J.S. Cho, S.K. Koh, D. Kim, *Thin Solid Films* 449 (2003) 147.
- [4] Y.B. Guo, C.N.F. Hong, *Diamond Relat. Mater.* 12 (2003) 946.
- [5] J.D. Mackenzie, E. Bescher, *J. Sol–Gel Sci. Technol.* 27 (2003) 7.
- [6] X. Zhang, Y. Wu, S. He, D. Yang, *Surf. Coat. Technol.* 201 (2007) 6051.
- [7] T.P. Chou, G. Cao, *J. Sol–Gel Sci. Technol.* 27 (2003) 31.
- [8] J.M. Urreaga, M.C. Matias, V. Lorenzo, M.U. Orden, *Mater. Lett.* 45 (2000) 293.
- [9] W. Tanglumert, P. Prasassarakich, P. Supaphol, S. Wongkasemjit, *Surf. Coat. Technol.* 200 (2006) 2784.
- [10] S. Pellice, P. Galliano, Y. Castro, A. Duran, *J. Sol–Gel Sci. Technol.* 28 (2003) 81.
- [11] A. Baraldi, R. Capelletti, M. Casalboni, C. Mora, M. Pavesi, R. Pizzoferrato, P. Prossposito, F. Sarcinelli, *J. Non-Cryst. Solids* 317 (2003) 231.
- [12] S. Sepeur, N. Kunze, B. Werner, H. Schmidt, *Thin Solid Films* 351 (1999) 216.
- [13] S.R. Davis, A.R. Brough, A. Atkinson, *J. Non-Cryst. Solids* 315 (2003) 197.
- [14] A. Kaminska, H. Kaczmarek, J. Kowalonek, *Eur. Polym. J.* 38 (9) (2002) 1915.
- [15] P. Munzert, U. Schulz, N. Kaiser, *Surf. Coat. Technol.* 174–175 (2003) 1048.
- [16] S. Vallon, B. Drevillon, C. Senemaud, A. Gheorghiu, V. Yakovlev, *J. Electron Spectrosc. Relat. Phenom.* 64/65 (1993) 849.
- [17] M.N. Sathyanarayana, M. Yaseen, *Prog. Org. Coat.* 26 (1995) 275.
- [18] J.D. Mackenzie, E. Bescher, *J. Sol–Gel Sci. Technol.* 27 (2002) 7.
- [19] C. Li, G.L. Wilkes, *J. Inorg. Organomet. Polym.* 8 (1998) 33.
- [20] C. Li, G.L. Wilkes, *J. Inorg. Organomet. Polym.* 7 (1997) 4.
- [21] D. mann, J. Fessmann, G. Kampschulte, M. Hopkins, *Surf. Coat. Technol.* 49 (1991) 168.
- [22] L.Y.L. Wu, E. Chwa, Z. Chen, X.T. Zeng, *Thin Solid Films*, 516 (2008) 1056.
- [23] ASTM D3359-02, *Standard Test Methods for Measuring Adhesion by Tape Test*, ASTM International, 2002.
- [24] ASTM D3363-00, *Standard Test Method for Film Hardness by Pencil Test*, ASTM International, 2000.
- [25] W.C. Oliver, G.M. Pharr, *J. Mater. Res.* 19 (2004) 3.
- [26] B.A. Latella, G. Triani, Z. Zhang, K.T. Short, J.R. Bartlett, M. Ignat, *Thin Solid Films* 515 (2007) 3138.
- [27] B.A. Latella, M. Ignat, C.J. Barbe, D.J. Cassidy, H. Li, *J. Sol–Gel Sci. Technol.* 31 (2004) 143.
- [28] L. Shapiro, S. Marx, D. Mandler, *Thin Solid Films*, 515 (2007) 4624.
- [29] F. Cardarelli (Ed.), *Materials Handbook: A Concise Desktop Reference*, 2nd Edition, Springer, 2008.